Grid-forming Control for Power Converters Based on Hybrid Energy Storage Systems during Islanding Operation

Hung Van NGUYEN [1], Chuong Trong TRINH [1], Giang Hoang VU [2], Huy Van BUI [1], Minh Duc NGUYEN [3], Son Hong NGUYEN [1], Duc-Cuong QUACH [1], Nghia Trong HOANG [4]*

[1] Hanoi University of Industry, Cau Dien 298, Hanoi, Vietnam
[2] Electric Power University, Hoang Quoc Viet 235, Hanoi, Vietnam
[3] Vietnam Academy of Science and Technology, Hoang Quoc Viet 18, Hanoi, Vietnam
[4] Ha Noi Open University, B101 Nguyen Hien, Hai Ba Trung, Hanoi, Vietnam

hung_nv@haui.edu.vn, chuongtt@haui.edu.vn*, giangvh@epu.edu.vn, ducminh.ies@gmail.com, htnghia2@hou.edu.vn

Submitted June 18, 2024/ Accepted September 11, 2024 / Online first November 4, 2024

Abstract. *Energy storage systems are increasingly playing a pivotal role in power systems. The combination of distributed sources and energy storage systems with local loads forms an autonomous distribution grid (ADG) capable of flexibly operating in either islanding or grid-connected modes. It is essential to maintain the state variables of the grid, such as frequency and voltage, within permitted ranges during the islanding mode, where the power converter control plays the most important role in the system operation. This paper proposes a control method for the power converter associated with a hybrid energy storage system (ESS) that is capable of forming the distribution grid during the islanding mode as well as following to the grid in grid-connected mode. The control method is based on a centralized energy controller to distribute energy between a battery and a supercapacitor. Accordingly, two voltage and current control loops using a PI hybrid fuzzy controller are designed. Simulation is developed using Matlab/Simulink software for a case study of a distribution network to illustrate the efficiency of the proposed control method.*

Keywords

Converters, energy storage systems, power distribution networks, supercapacitor

1. Introduction

In recent years, energy storage devices and systems have gradually become a trend and played an important role in grid-connected or standalone power systems. ESS technology has become popular due to several advantages and benefits, including ensuring backup energy storage, improving power supply reliability in the power system, and helping to diversify the way the grid operates in unusual situations. A typical ESS today is the traditional battery energy storage system (BESS), which has the outstanding characteristic and advantage of large energy storage capacity. The application of BESS allows for improving energy efficiency by storing excess energy for later use utilization, reducing energy waste and increasing the efficiency of the entire power system. In addition, with compactness and unlimited installation locations, battery energy storage systems are easy to install in many different regions without dependence on other energy sources. However, a BESS requires a certain amount of time to respond to power changes and the limitation of injecting power into the main grid may affect the performance of the system [1], [2].

Similar to BESS system, current supercapacitors also offer several benefits in the power system. Supercapacitors are capable of serving the short-term needs of power, helping to ensure a stable power supply in a short time [3], [4]. Furthermore, supercapacitors have high operational efficiency, ensuring a stable power supply and prompt response to the requirements of power systems. However, supercapacitors have lower energy storage capacity than traditional ESSs or batteries. Therefore, supercapacitors are only suitable for applications with low and short-term energy requirements, and cannot completely replace traditional ESSs. To overcome this drawback, supercapacitors can be integrated with other types of ESSs as a solution to increase efficiency and reduce power loss during energy conversion and storage [5]. Optimizing the operation of the ESS is the initial solution to be applied and gives feasible results in ensuring the stability of the system. Most current studies apply ESSs in order to reduce peak load and improve the flexibility of the grid system without emphasizing the efficiency and reliability of the grid system in a short time and minimizing incidents [6], [7].

In order to meet the energy needs of the power system quickly, increase the efficiency and ensure the stability of

DOI: 10.13164/re.2024.0660

frequency and voltage, the paper proposes a method of controlling the grid-holding inverter in the islanding distribution grid based on a battery-supercapacitor hybrid ESS. The remainder of the article is organized as follows: Section 2 presents the model of main elements in a case study of a distribution network. A control method based on fuzzy logic for the allocation of power between BESS and supercapacitor is then introduced in Sec. 3. In Sec. 4, simulations are carried out in Matlab/Simulink tool to highlight the effectiveness of the proposed control method.

2. System Components Modelling

2.1 Traditional ESS

Electrical energy storage technology is evolving and continually improving to meet the growing demands of the power and energy sector. In particular, batteries are the most popular electrical energy storage technology today. There are different types of batteries that are commonly used today, such as lithium-ion batteries, lead-acid batteries, and sodium-sulfur batteries. Among these, lithium-ion batteries provide relatively good performance, with high power density and energy density; long life cycles without memory effects, large amounts of energy storage in a small space, low self-discharge rates, and the capability of being recharged multiple times before starting to degrade [8].

As a matter of fact, the lithium-ion battery is a preferred option for energy storage and is the most popular battery type today. Therefore, this type of battery is selected in this study as a representative of traditional ESS. Following this, the mathematical model of a BESS is introduced, including a Thevenin equivalent circuit to characterize the voltage-current characteristics, and a time equivalent circuit to describe the lifespan, capacity, state of charge (SOC), and operating time. Mathematical models that can predict the operation of ESS in power systems offer tailored solutions to improve ESS performance and service life. Figure 1 and Figure 2 show two equivalent circuits of the BESS [9].

The mathematical model characterizes battery life, capacity, SOC, and runtime through three parameters as shown in Fig. 1, including a resistor R_{self}, representing the energy self-discharge lost during storage; a current source dependent on current for charging and discharging (I_{batt}) and a capacitor (C_{cap}) giving the state of the battery as a voltage drop value, $V_{\text{SOC}} \in [0, 1]$ [10], [11].

The C_{cap} charge value characterizes the entire charge stored in the battery and can be calculated as follows [12]:

$$C_{\text{cap}} = 3600 C_{\text{n}} f_1(T) f_2(n) f_3(i) \tag{1}$$

in which, C_{n} is the rated battery capacity (Ah); $f_1(T)$, $f_2(n)$ and $f_3(i)$ are the temperature-dependent adjustment factors, the number of cycles and the corresponding current, respectively.

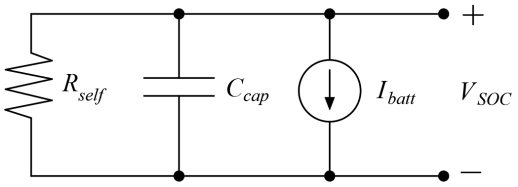

Fig. 1. The model's determination of battery life.

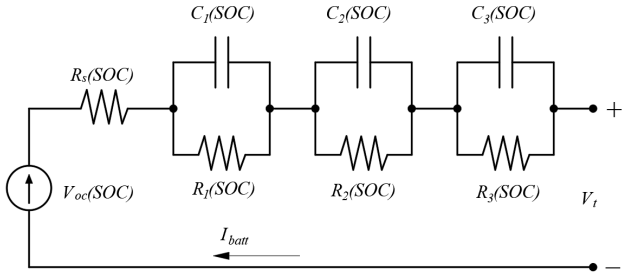

Fig. 2. Battery V-I characteristics model.

The characteristic model for the voltage-current relationship of a battery, represented by an equivalent circuit, is depicted in Fig. 2. In this case, all elements of the equivalent circuit depend on the SOC. The non-linear voltage-current relationship is integrated through a voltage-dependent power supply (V_{o}), and a resistance (R_{s}) is responsible for the voltage change. Some parallel *RC* circuits, including R_{i} and C_{i}, are connected in series to provide different time constants. The parameters defined in Fig. 2 are functions of the SOC, expressed through the following equations, and they are also influenced by other operating characteristics such as temperature.

$$SOC(t) = SOC_0 - \frac{1}{C_{\text{cap}}} \int_0^1 i(t)\,\mathrm{d}t, \tag{2}$$

$$V_{\text{t}} = V_{\text{oc}}\left(SOC, T\right) - i_{\text{bat}}\left(t\right) R_{\text{bat}}\left(SOC, T\right) + i_{\text{bat}}\left(t\right) R_{\text{t}}, \tag{3}$$

$$R_{\text{t}} = \left(R_1\left(SOC\right)\right) \mathrm{e}^{\frac{-1}{R_1(SOC)C_1(SOC)}t} + \left(R_2\left(SOC\right)\right) \mathrm{e}^{\frac{-1}{R_2(SOC)C_2(SOC)}t} + \left(R_3\left(SOC\right)\right) \mathrm{e}^{\frac{-1}{R_3(SOC)C_3(SOC)}t} \tag{4}$$

in which, V_{C1}, V_{C2} and V_{C3} are the voltage across the capacitors, V_{Rs} are voltage drop across internal resistance R_{s}.

2.2 Supercapacitor

A supercapacitor is a type of polarized capacitor that uses an electrolyte instead of a dielectric. It is capable of storing energy, charging/discharging quickly, and providing high energy in a very short time. Additionally, it can be deeply discharged without affecting its lifespan, which is not true for lead-acid and Li-ion batteries. Supercapacitors are divided into three types: electrostatic double-layer capacitors, electrochemical pseudo capacitors, and hybrid supercapacitors. They are particularly suitable for applications that require high power supply speeds and short cycles, such as hybrid electric vehicles, voltage-assisted ap-

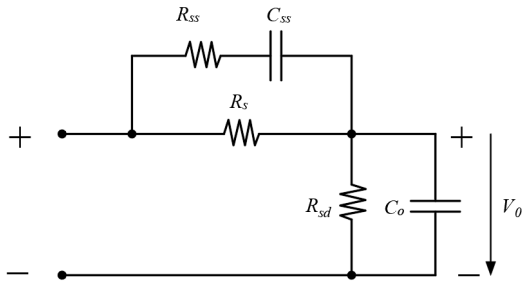

Fig. 3. Supercapacitor substitution model.

plications in DC converters, and power quality correction in utility applications. The equivalent circuit of a supercapacitor is presented in Fig. 3 [13].

Models of supercapacitors often use passive elements such as resistors and capacitors. The self-discharge of the capacitor is characterized by R_{sd}. The cell resistance and the splice resistance are replaced by R_s (series resistance) and RC elements, R_{ss} and C_{ss} elements characterize the transient characteristics [14]. The capacitance of a supercapacitor is calculated by:

$$C_c(V_{0i}) = \frac{\Delta Q_i}{\Delta V_{0i}} = \frac{\sum_i I_i(t)\Delta t}{\Delta V_{0i}} \tag{5}$$

in which, C_c (V_{0i}) is the internal capacitance at point i; I_i is the proportional current at point i; Q_i is the charge of the i^{th} storage point.

2.3 Bidirectional DC-DC Power Converter

A bidirectional DC-DC power converter acts as an input voltage transformer and as a charging circuit for batteries and supercapacitors. In addition, it stabilizes the DC voltage for the input of a DC-AC power converter [15], [16].

When discharging, the circuit operates in two modes: continuous mode and intermittent mode. In continuous current mode, the energy accumulated in the inductor is enough to maintain the current to the next closing/cutting cycle, resulting in an output voltage that is greater than the input voltage. The output voltage of the converter is [16]:

$$V_{out} = \frac{1}{1-k} V_{in}. \tag{6}$$

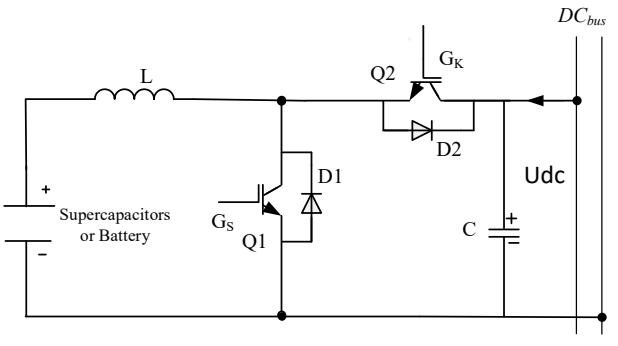

Fig. 4. Bidirectional DC-DC power converter.

In discontinuous current mode the output voltage of the converter is:

$$V_{in}kT + (V_{in} - V_{out})\Delta_1 T = 0, \tag{7}$$

$$V_{out} = \frac{\Delta_1 + k}{\Delta_1} V_{in}. \tag{8}$$

In this context, V_{out} and V_{in} respectively are the output and input voltages of the converter, respectively; k is the duty cycle; T is the switching time; and Δ_1 is the negative inductor voltage interval. The capacitor charge and discharge process is determined by the following equation:

$$\frac{C}{2}\frac{\mathrm{d}v_{dc}^{\ 2}}{\mathrm{d}t} = P_{BESS} - P_{AC}, \tag{9}$$

$$P_{AC} = \frac{3}{2}(v_d i_d + v_q i_q) \tag{10}$$

ESS operation mode [17], where:

Discharge mode:

$$V_{batt} = E_0 - Ri - K\frac{Q}{Q-it}(it + i^*) + A\mathrm{e}^{(-Bit)} \tag{11}$$

Charge mode:

$$V_{batt} = E_0 - Ri - K\frac{Q}{it-0.1Q}i^* - K\frac{Q}{Q-it}it + \mathrm{e}^t \tag{12}$$

in which, V_{batt} and E_0 represent the battery voltage and the constant battery voltage, respectively, and i and i^* denote the battery current and filtered current.

In what follows, the general design plan for the Fuzzy-PI controller will be introduced. The bidirectional DC-DC converter system is connected to the power storage system (supercapacitor, battery). Using a traditional PI control structure can lead to control quality that does not sufficiently meet the desired requirements [18–20].

In this paper, we propose a hybrid PI-fuzzy controller, shown in Fig. 5, to replace traditional PI controllers. Thus, the DC-DC control system is a two-loop structure of voltage and current control using a PI-fuzzy hybrid controller.

The controller generates control signal $u = u_f + u_p$, where u_f is the output component of the blur processing stage. The inputs of this fuzzy processing step includes an error e and an error derivative de/dt. The blur processing stage is shown in Fig. 6, including:

- Input fuzzification: the error e is fuzzified into 5 fuzzy sets {BNe, Ne, Ze, Pe, BPe}, the error derivative e is fuzzified into 3 fuzzy sets {Nd, Zd, Pd}. Membership functions typed isosceles triangle are used.

- The output fuzzy set y uses an isosceles triangle membership function including 5 fuzzy sets {B, N, Z, P, BP}.

- Use Max-PROD composition argument, 15 fuzzy rules are applied as shown in Fig. 6. The fuzzy rules are

formed according to logics: when the error is 0, the output u_f remains unchanged; when the error is positive (the reference value is greater than the measured value of the quantity to be controlled), the amount u needs to be increased. On the contrary, when the error is negative, the amount of u_f is reduced.

- Defuzzification is implemented by using the center of gravity method. The output component u_f is calculated by:

$$u_f = \frac{\int y\mu_y(y)\mathrm{d}y}{\int \mu_y(y)\mathrm{d}y} \tag{13}$$

where μ_y is the output of membership function. The blurred surface in relative units is shown in Fig. 7.

The control value of the Fuzzy-PI controller given in the diagram in Fig. 6 is applied to the DC-DC converter control structure, which is determined by:

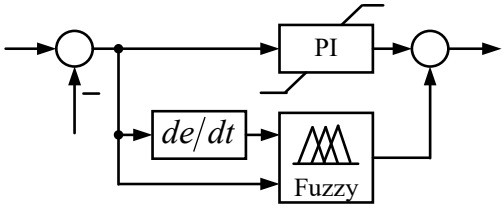

Fig. 5. Hybrid fuzzy controller PI (Fuzzy-PI).

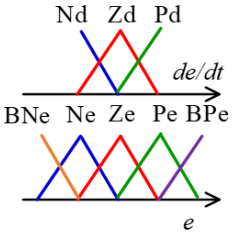

Max-PRO

e' \ e	BNe	Ne	Ze	Pe	BPe
Pd	N	Z	Z	P	BP
Zd	N	Z	Z	Z	P
Nd	BN	N	Z	Z	P

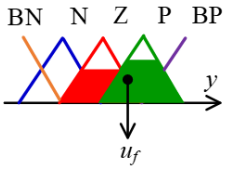

Fig. 6. Structure of the blur processing stage.

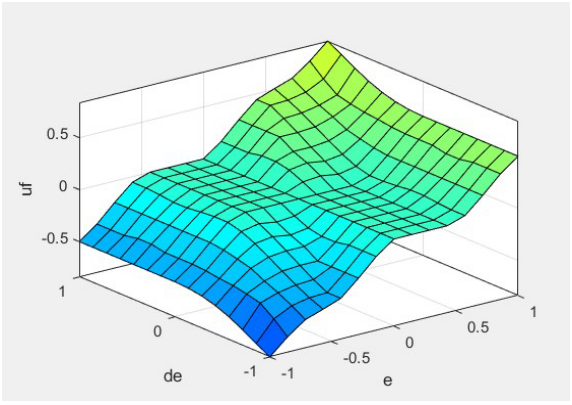

Fig. 7. Fuzzy surface characteristics designed for the fuzzy processing stage of the Fuzzy-PI set.

Parameters		Fuzzy-PI controller for voltage control loop	Fuzzy-PI controller for current control loop
Input fuzzification	Number of inputs	2	2
	Input error	5 fuzzy sets, function in the form of an equilateral triangle, error range [–100, 100] V, fuzzy sets {BNe, Ne, Ze, Pe, BPe}	5 fuzzy sets, function in the form of an equilateral triangle, error range [–15, 15] A, fuzzy sets {BNe, Ne, Ze, Pe, BPe}
	Error derivative input	3 fuzzy sets, function in the form of an equilateral triangle, error range [–500, 500] V/s, fuzzy sets {Nd, Zd, Pd}	3 fuzzy sets, function in the form of an equilateral triangle, error range [–100, 100] A/s, fuzzy sets {Nd, Zd, Pd}
Output fuzzification	Number of outputs	1	1
	Fuzzification	5 fuzzy sets, function in the form of an equilateral triangle, value range [0, 1], fuzzy sets {B, N, Z, P, BP}	5 fuzzy sets, function in the form of an equilateral triangle, value range [0, 1], fuzzy sets {B, N, Z, P, BP}
Law of composition		Max-PROD	Max-PROD
Fuzzy law		Figure 7	Figure 7

Tab. 1. Parameters of Fuzzy-PI controllers.

$$u = u_p + u_f,$$
$$u = K_p e + K_i \int_0^t e(\tau)\mathrm{d}\tau + \frac{\int y\mu_y(y)\mathrm{d}y}{\int \mu_y(y)\mathrm{d}y}. \tag{14}$$

The Fuzzy-PI controller reference for the current and voltage control loops is given in Tab. 1.

2.4 The DC-AC Converter

The DC-AC converter converts DC power from the energy accumulated in the battery pack and supercapacitor into AC power to supply the loads. It is capable of generating an output AC signal with custom voltages and frequencies to suit different loads. The DC-AC converter has a dual-loop control structure. The external control loop is responsible for controlling DC voltage and reactive power, while the internal control loop is responsible for controlling the current. This loop controls the output voltage of the converter using a PI controller designed on the perpendicular rotation axis dq. A phase lock loop (PLL) circuit is used to maintain synchronization between the input signal and the output signal and to calculate the phases of the AC. The converter is connected to the main grid via an LCL filter, as shown in Fig. 8. The voltage equation of the PI controller is proposed as:

$$\begin{cases} u_d^* = e_d - \omega L i_q + (k_p + \dfrac{k_i}{s})(i_{dref} - i_d) \\ u_q^* = e_q + \omega L i_d + (k_p + \dfrac{k_i}{s})(i_{dref} - i_q) \end{cases} \tag{15}$$

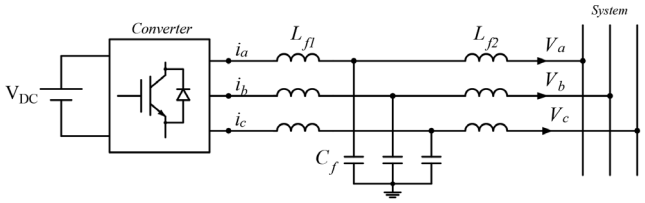

Fig. 8. The circuit of DC-AC converter with an LCL filter.

2.5 Control Structure Based on Current and Voltage Transducers

The system's controller utilizes a dual-loop control structure for managing current and voltage. This design ensures that both frequency and voltage requirements are met. The two control loops generate respective signals to manage the charging and discharging processes of the battery and capacitor during power supply disconnection and reconnection, as illustrated in Fig. 9 and Fig. 10.

In Fig. 9, the output of the external voltage controllers is used as the reference currents for the internal current control loops, i.e.:

$$i_{\text{dref1}} = i_{\text{Ld1}} + (V_{\text{dref1}} - V_{\text{d}})\frac{k_{\text{pd}} + k_{\text{id}}}{s} - V_{\text{q}}\omega C, \tag{16}$$

$$i_{\text{qref1}} = i_{\text{Lq1}} + (V_{\text{dref1}} - V_{\text{q}})\frac{k_{\text{pq}} + k_{\text{iq}}}{s} - V_{\text{d}}\omega C, \tag{17}$$

$$\theta = \int \left[\omega^* + \left(P^* - P\right)m_{\text{P}}\right]\text{d}t. \tag{18}$$

The design of controllers for the DC voltage and powers is adopted from [21], [22]. As a result, the parameters of controllers can be obtained and provided in Tab. 2. Simulation results of the ADG operating with the traditional PI controllers will be used as reference to compare with those of hybrid PI controller in Sec. 4.

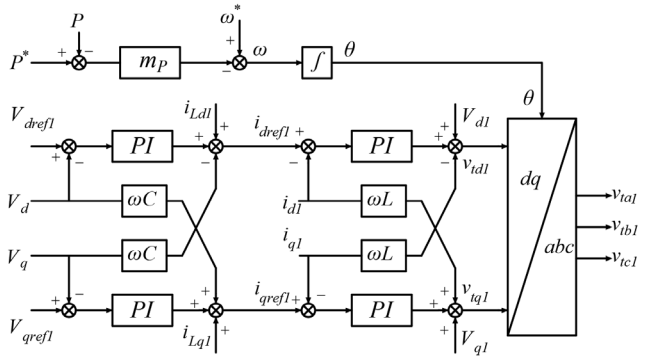

Fig. 9. Grid retaining mode transformer control schematic.

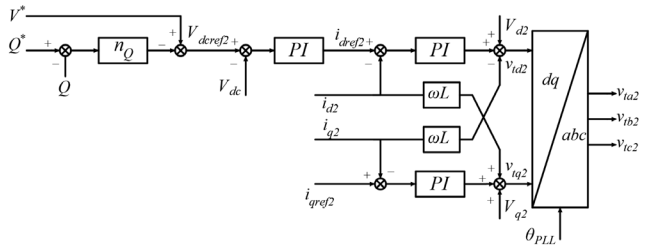

Fig. 10. Grid traction converter control scheme.

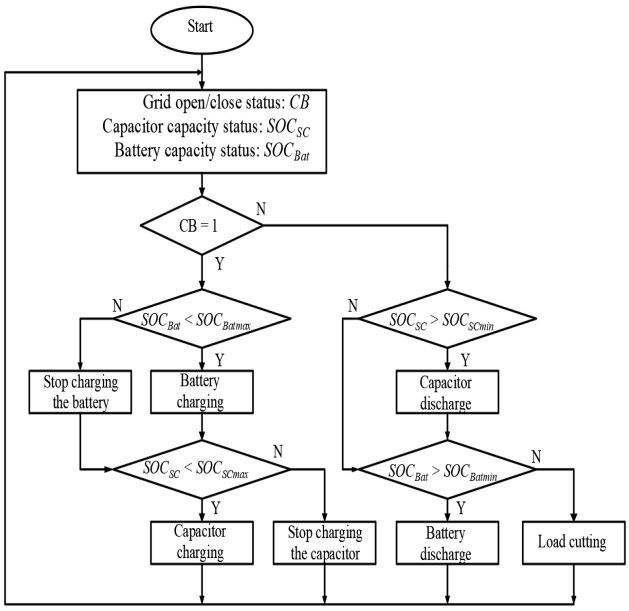

Fig. 11. Diagram of control algorithm for power allocation.

3. Power Allocation Control between ESS and Supercapacitor

The control strategy of battery and supercapacitor in both charging and discharging modes is proposed with control algorithm provided in Fig. 11. In Fig. 11, SOC_{Batmax} and SOC_{Batmin} are the maximum and minimum capacities of ESS, respectively; SOC_{SCtmax} and SOC_{SCtmin} are the maximum and minimum capacities of the capacitor, respectively.

In grid-connected mode, PCC = 1, if the battery or supercapacitor capacities are not full, they will be charged until the maximum SOC is reached. When the distribution network is disconnected from the main grid, the supercapacitor will have the function of rapidly recovering the power supply to the load; meanwhile the battery simultaneously discharges to maintain the power supply to the load. In that situation, if the energy accumulated in both battery and supercapacitor is exhausted or below their SOC_{min}, the load sheading should be carried out and the battery or supercapacitor should be tripped to avoid damage. If the mains power is restored during the discharge, the cycle will be repeated as before.

4. Simulation Results

Application of a supercapacitor-BESS hybrid model to improvement of frequency and voltage is illustrated in this section. Simulation is carried out for an ADG operating in islanding mode, whose diagram is provided in Fig. 12. The ADG is composed of a BESS, a supercapacitor, and a DC-AC power converter, which are connected to a common DC bus. The AC side of the converter is used to supply two loads (Load 1 and Load 2) via distribution lines in a radial configuration. In addition, the ending node of

the line is the PCC with the main grid. The simulation is carried out for 10 seconds, using the parameters of the elements given in Tabs. 2 and 3. The ADG initially operates in grid-connected mode to supply load 1 (P = 150 kW, Q = 20 kVAr). Disturbances are then created by disconnecting the ADG from the main grid at t = 3 s and switching on Load 2 (P = 100 kW, Q = 20 kVAr) at t = 6 s. Finally, the main grid connection is recovered at t = 8 s. Hence, the simulation results in islanding mode will be observed from t = 3 s to t = 8 s.

Figure 13(a) and (b) respectively show the comparison of battery currents and state of charges (SOC_{Bat}) in two cases with and without using a supercapacitor. It is seen that the disturbances cause increases in battery current and decreases in SOC_{Bat} during the discharging operation. In such operation, the supercapacitor also discharges, as can be viewed in Fig. 14, and provides significant support by requiring smaller current and maintaining a higher level of SOC_{Bat} for the battery.

During the grid-connected mode, the battery and capacitor are charged, both adhering to the grid. After t = 3 s, the battery and supercapacitor start discharging operation, during which the battery plays the role of shaping, while the supercapacitor remains connected to the ADG.

The responses of grid frequency under disturbances due to the main grid disconnection and load increase are shown in Fig. 15. It is seen that the application of supercapacitor-BESS hybrid system gives a more stable frequency, improving frequency oscillation and frequency change rate to benefit the grid.

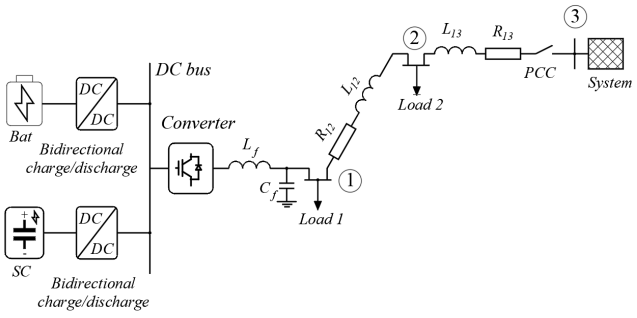

Fig. 12. Diagram of an autonomous distribution grid.

Parameter	Value	Parameter	Value
ESS voltage	500 V	Load 1	150 + j20 kVA
ESS capacity	500 Ah	Load 2	100 + j20 kVA
Supercapacitor voltage	600 V	Supercapacitor capacity	20 F

Tab. 2. Grid and load parameters.

Parameter	Value	Parameter	Value
L_{fl}	0.17 mH	k_{pd}	0.6
R_{fl}	0.54 mΩ	k_{id}	10^4
C_{fl}	10 mF	k_{pq}	–0.03
k_{pv}	2.5	k_{iq}	–55
k_{iv}	100	k_{pc}	2.5
T_d	0.01 s	k_{ic}	625

Tab. 3. Control parameters.

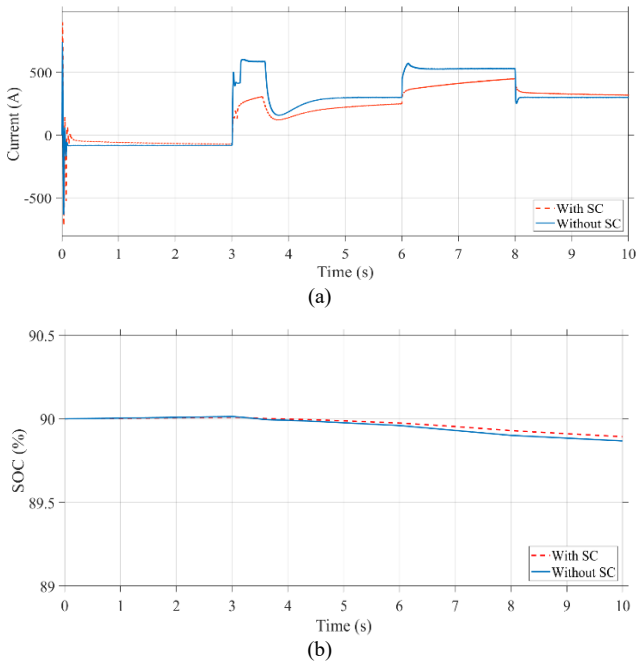

Fig. 13. Comparison of the current (a) and SOC (b) of battery between two cases with and without supercapacitor (SC).

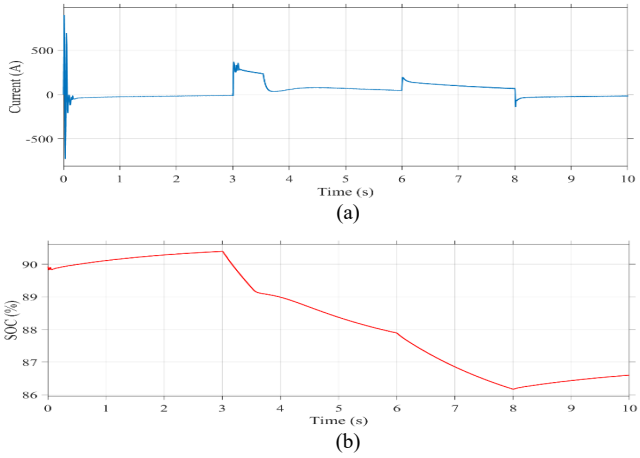

Fig. 14. Characteristics of the supercapacitor current (a) and SOCSC (b).

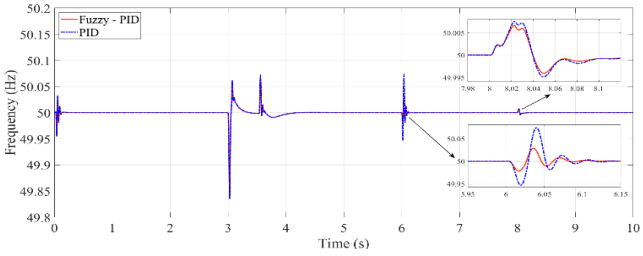

Fig. 15. Comparison of the frequency responses.

In what follows, a simulation is further developed that a main grid disconnection at t = 3 s and sudden change in load capacity at t = 6 s, i.e., the active power of load 1 is increased from 150 kW to 250 kW. It can be observed in Fig. 16 and Fig. 17 that the output powers of the BESS and supercapacitor fluctuates due to the disturbances caused by

the main grid disconnecting and the load increase, in order to guarantee the power balance in the grid. It was found that when applying the supercapacitor-BESS hybrid model, the active power and reactive power were rapidly stabilized. The current response during the disconnecting of the main grid is depicted in Fig. 18. It is evident that the inclusion of supercapacitors aids in rapidly stabilizing current fluctuations, allowing the system to achieve a steady state more efficiently.

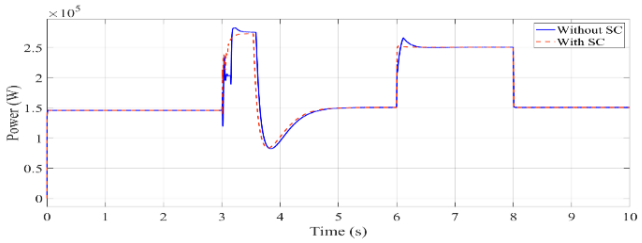

Fig. 16. Comparison of active powers of BESS.

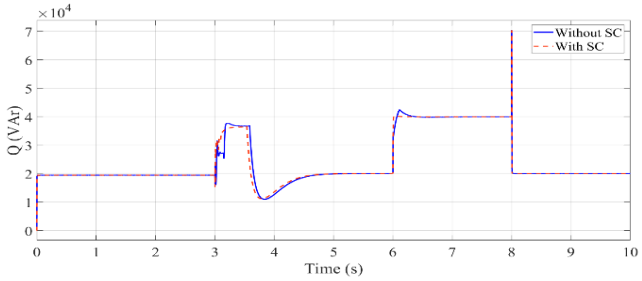

Fig. 17. Comparison of reactive powers of BESS.

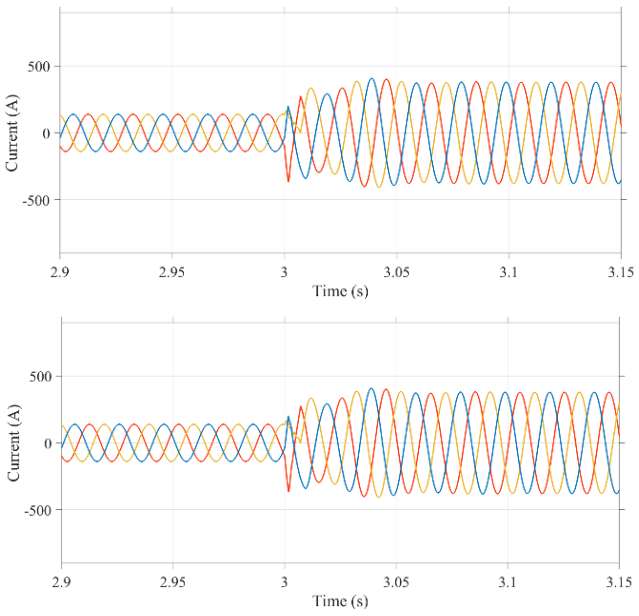

Fig. 18. The current during the disconnecting of the main grid.

Figures 19, 20 and 21 show the responses of current and voltage during the main grid disconnection ($t = 3$ s) and sudden change of the load ($t = 6$ s). Owing to the operation of the control loops of the converter and that of the BESS-supercapacitor system, the grid voltage is kept stable within the permitted limit before the intervention of the next control levels.

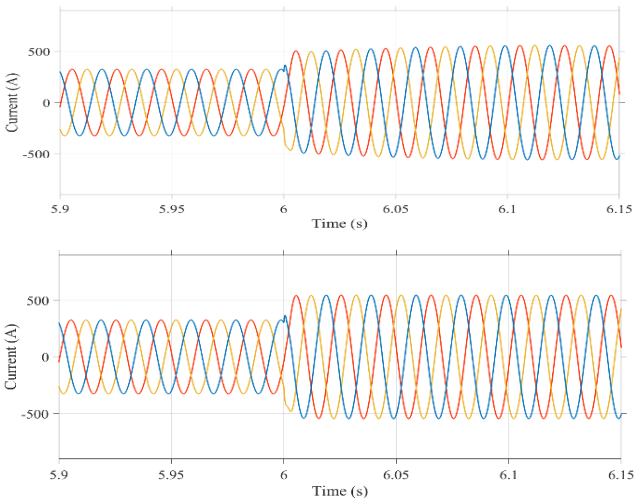

Fig. 19. Current variation under a sudden change of load.

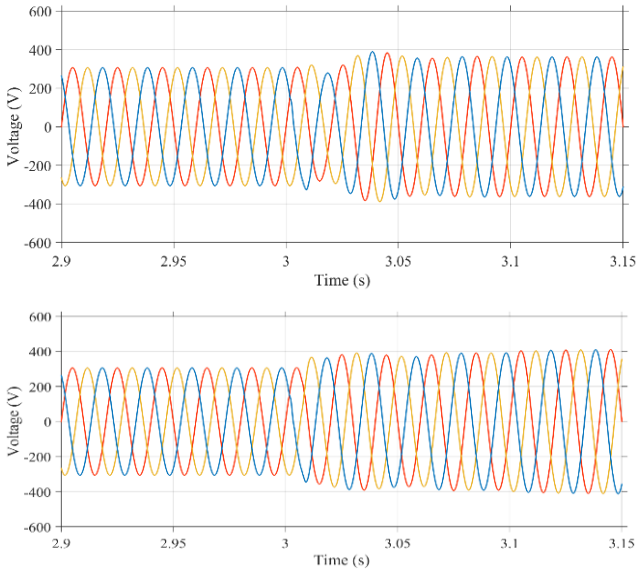

Fig. 20. Grid voltage variation during main grid disconnection.

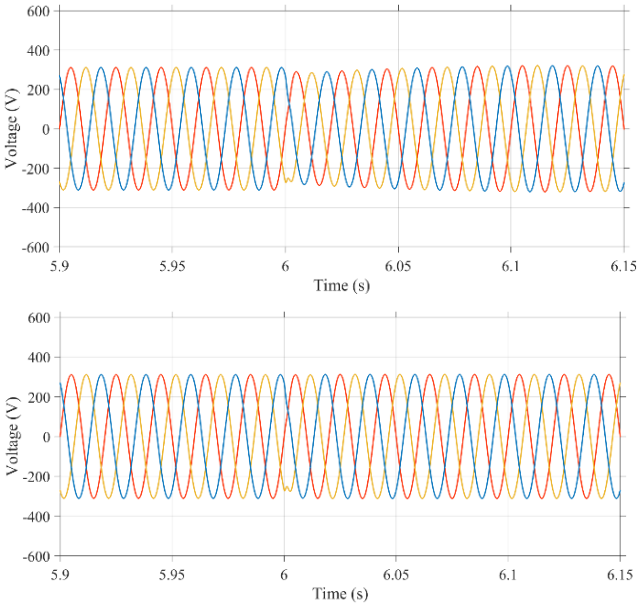

Fig. 21. Grid voltage under a sudden change of load.

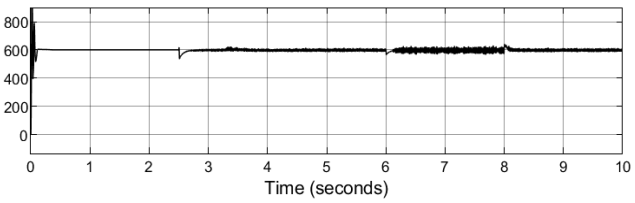

Fig. 22. DC voltage on DC bus.

The results in Fig. 22 show that the DC bus voltage is maintained at 600 V, demonstrating that the energy exchange process is balanced even when there are fluctuations in load or changes in the system's working conditions.

Thus, it can be seen that by exploiting the advantages of BESS and supercapacitor energy storage forms, along with the application of controllers based on fuzzy logic algorithms, the frequency and voltage of the ADG have been sufficiently maintained in the grid islanding mode.

5. Conclusions

The solution using a BESS-supercapacitor hybrid system for the purpose of improving the frequency and voltage of the grid independently of the photovoltaic system is proposed in this paper. The paper also conducted simulations to validate the proposed control model. When there are factors that change the active power balance, causing a change in frequency, the simulation results show that the proposed control model provides effective responses to the charging and discharging processes of the battery and supercapacitor. As a result, the amplitude and frequency change rates have been significantly improved.

In addition to the successful demonstration of frequency and voltage regulation, future research could focus on further optimizing the control algorithms to enhance the efficiency and response times of the system. Exploring the integration of other renewable energy sources, such as wind power, with the BESS-supercapacitor hybrid system could also provide a more robust solution for grid stability. Furthermore, real-world testing and validation of the proposed model under various operational conditions would be crucial in advancing the practical application of this technology. Potential development may include the creation of scalable models that can be adapted for different grid sizes and configurations, thereby broadening the applicability and impact of this solution.

Acknowledgment

This paper was conducted with funding support from the independent science and technology project at the level of the Vietnam Academy of Science and Technology. Code: ĐL0000.01/22-23.

Conflicts of Interest

The authors declare that they have no conflicts of interest.

References

[1] MESBAHI, T., RIZOUG, N., BARTHOLOMËUS, P., et al. Dynamic model of Li-ion batteries incorporating electrothermal and ageing aspects for electric vehicle applications. *IEEE Transactions on Industrial Electronics*, 2018, vol. 65, no. 2, p. 1298–1305. DOI: 10.1109/TIE.2017.2714118

[2] ABU-SHARKH, S., DOERFFEL, D. Rapid test and non-linear model characterisation of solid-state lithium-ion batteries. *Journal of Power Sources*, 2004, vol. 130, no. 1–2, p. 266–274. DOI: 10.1016/j.jpowsour.2003.12.001

[3] ERAGAMREDDY, G., NAIK, S. G. Power management system for a hybrid energy storage electric vehicle using fuzzy logic controller. *Bulletin of Electrical Engineering and Informatics*, 2024, vol. 13, no. 3, p. 1443–1452. DOI: 10.11591/eei.v13i3.6608

[4] ALI, M., HOSSAIN, M. I., SHAFIULLAH, M. Fuzzy logic for energy management in hybrid energy storage systems integrated DC microgrid. In *2022 International Conference on Power Energy Systems and Applications (ICoPESA 2022)*. Nanjing (China), p. 424–429. DOI: 10.1109/ICoPESA54515.2022.9754406

[5] ARIYARATHNA, T., JAYANANDA, D., KULARATNA, N., et al. Potential of supercapacitors in novel power converters as semi-ideal lossless voltage droppers. In *43rd Annual Conference of the IEEE Industrial Electronics Society (IECON)*. Bejing (China), 2017, p. 1429–1434. DOI: 10.1109/IECON.2017.8216243

[6] CHOI, S. C., JEON, J. Y., YEO, T. J., et al. State-of-charge balancing control of a battery power module for a modularized battery for electric vehicle. *Journal of Electrical Engineering and Technology*, 2016, vol. 11, no. 3, p. 629–638. DOI: 10.5370/JEET.2016.11.3.629

[7] CASTILLO, A., GAYME, D. F. Grid-scale energy storage applications in renewable energy integration: A survey. *Energy Conversion and Management*, 2014, vol. 87, p. 885–894. DOI: 10.1016/j.enconman.2014.07.063

[8] AKHIL, A. A., HUFF, G., CURRIER, A. B., et al. *DOE/EPRI Electricity Storage Handbook in Collaboration with NRECA*. 2015, p. 1–347. [Online] Cited 2024-06-18. Available: http://www.sandia.gov/ess/publications/SAND2015-1002.pdf

[9] CAO, J., HARROLD, D., FAN, Z., et al. Deep reinforcement learning based energy storage arbitrage with accurate lithium-ion battery degradation model. *IEEE Transactions on Smart Grid,* 2020, vol. 11, no. 5, p. 4513–4521. DOI: 10.1109/TSG.2020.2986333

[10] PETRZELA, J. Accurate constant phase elements dedicated for audio signal processing. *Applied Sciences*, 2019, vol. 9, no. 22, p. 1–38. DOI: 10.3390/app9224888

[11] PETRZELA, J. Fractional-order chaotic memory with wideband constant phase elements. *Entropy*, 2020, vol. 22, no. 4, p. 1–32. DOI: 10.3390/E22040422

[12] HAMIDI, A., WEBER, L., NASIRI, A. EV charging station integrating renewable energy and second-life battery. In *2013 International Conference of Renewable Energy Resources and Applications (ICRERA 2013)*. Madrid (Spain), 2013 p. 1217–1221. DOI: 10.1109/ICRERA.2013.6749937

[13] BERTRAND, N., SABATIER, J., BRIAT, O., et al. Embedded fractional nonlinear supercapacitor model and its parametric

estimation method. *IEEE Transactions on Industrial Electronics*, 2010, vol. 57, no. 12, p. 3991–4000. DOI: 10.1109/TIE.2010.2076307

[14] MANLA, E., MANDIC, G., NASIRI, A. Testing and modeling of lithium-ion ultracapacitors. In *2011 IEEE Energy Conversion Congress and Exposition (ECCE 2011)*. Phoenix (AZ, USA), 2011, p. 2957–2962. DOI: 10.1109/ECCE.2011.6064167

[15] HAZRA, P. Enhancement of inertial response of inverter based energy system and its application for dynamic performance improvement of a microgrid. *M.Sc. Theses,* Clemson University, 2020, p. 1–211. [Online] Cited 2024-10-29. Available: https://open.clemson.edu/all_theses/3452/

[16] RUAN, X., LI, B., CHEN, Q., et al. Fundamental considerations of three-level DC-DC converters: Topologies, analyses, and control. *IEEE Transactions on Circuits and Systems I: Regular Papers*, 2008, vol. 55, no. 11, p. 3733–3743. DOI: 10.1109/TCSI.2008.927218

[17] TREMBLAY, O., DESSAINT, L. A. Experimental validation of a battery dynamic model for EV applications. *World Electric Vehicle Journal,* 2009, vol. 3, no. 2, p. 289–298. DOI: 10.3390/wevj3020289

[18] ŞEN, M., ÖZCAN, M., EKER, Y. R. Fuzzy logic-based energy management system for regenerative braking of electric vehicles with hybrid energy storage system. *Applied Sciences*, 2024, vol. 14, no. 7, p. 1–25. DOI: 10.3390/app14073077

[19] BIEDKA, H., RAFAL, K. Control algorithms of hybrid energy storage system based on fuzzy logic. In *2021 Progress in Applied Electrical Engineering (PAEE 2021)*. Koscielisko (Poland), 2021, p. 1–5. DOI: 10.1109/PAEE53366.2021.9497387

[20] RAHMAN, A. U., ZEHRA, S. S., AHMAD, I., et al. Fuzzy supertwisting sliding mode-based energy management and control of hybrid energy storage system in electric vehicle considering fuel economy. *Journal of Energy Storage*, 2021, vol. 37, p. 1–14. DOI: 10.1016/j.est.2021.102468

[21] VU, H.-G. DC-link voltage control of voltage source converter by using PI controller with anti-windup (in Vietnamese). *Journal of Science and Technology University Da Nang*, 2018, vol. 11, no. 1, p. 18–21.

[22] VU, H. G., YAHOUI, H., CHOROT, T., et al. Control active and reactive power of Voltage Source Inverter (VSI). In *2nd International Symposium on Environment Friendly Energies and Applications (EFEA)*. Newcastle upon Tyne (UK), 2012, p. 308 to 311. DOI: 10.1109/EFEA.2012.6294057

About the Authors …

Hung Van NGUYEN is currently working at the Department of Power System, Hanoi Industrial University. He graduated from Hanoi University of Technology in 2011, major in Electrical System. In 2014, Hung obtained Master degree of Electrical Engineering at Hanoi University of Technology. His current main research are reliability in power system and distributed power generations.

Chuong Trong TRINH (*corresponding author) is currently working at the Faculty of Electrical Engineering, Hanoi University of Industry. Chuong graduated from Hanoi University of Science and Technology in 1999, major in Electrical System followed by a Master's degree and Ph.D. in Electrical Engineering in 2003 and 2012, respectively. Currently, he is an Associate Professor at Hanoi University of Industry, Vietnam. His current main research topic include: reconfiguration of the distribution network; voltage stabilization; power system operation and control and distributed generations.

Giang Hoang VU holds a Ph.D. in Electrical Engineering from University of Claude Bernard Lyon 1. He is currently Head of the Department of Power Plants and Substations at the Electric Power University. His research interests include condition monitoring and estimation of electrical machines and power electronics converter; and integration of renewable energy based power sources into the power grids.

Son Hong NGUYEN is currently studying at the Faculty of Electrical Engineering, majoring in Electrical and Electronics Engineering, Hanoi University of Industry.

Huy Van BUI is currently working in the Faculty of Electrical Engineering, Hanoi University of Industry. He graduated from Hanoi University of Science and Technology in 2005 with a degree in Control and Automation Engineering, earned his Master's degree in 2008, and obtained his Ph.D. in Control and Automation Engineering from Hanoi University of Science and Technology in 2017. His research focuses on automation in power systems, power electronics and applications in renewable energy sources.

Minh Duc NGUYEN is currently Director of the Research Center for Sustainable Energy Development and a principal researcher of the Institute of Energy Sciences, Vietnam Academy of Science and Technology. He graduated from the University of Science and Technology in 2004, he received a Master's degree in Electrical Systems and Automation from Kunming University of Technology, China in 2012, a Ph.D. in Electrical Engineering from the Hanoi University of Mining and Geology in 2023. His research sectors are research and application of energy technology deployment in civil, industrial, and agricultural; energy and environment impact research; new energy research, renewable energy; energy security.

Duc-Cuong QUACH received the B.S. degree in Electrical Machines and Power Electronics from Hanoi University of Science and Technology, M.S. degree in Automation Engineering from Ho Chi Minh City University of Transport (Vietnam), and Ph.D. degree in Control Science and Control Engineering from Huazhong University of Science and Technology (Wuhan, PR China) in 2002, 2008 and 2013. He is currently working at the Faculty of Electrical Engineering Technology, Hanoi University of Industry, Vietnam. His research interests include wireless sensor networks, intelligent control theories and embedded systems applied to power electronics-electrical drives, solar energy control systems and industrial applications.

Nghia Trong HOANG received his master's degree in Electronic Engineering in 2018 at the Electric Power University. Currently, he is an expert at the Vietnam. He is a Lecturer with the Faculty of Electrical and Electronic Engineering, Hanoi Open University. His research interests include internet; network protocol; network security; WSN; IoT.